AD-A131 632 THE EFFECTS OF SMALL NOISE ON IMPLICITLY DEFINED NON-LINEAR DYNAMICAL SYS..(U) MASSACHUSETTS INST OF TECH CAMBRIDGE LAB FOR INFORMATION AND D.. S SASTRY 1/1

UNCLASSIFIED SEP 82 LIDS-P-1249 AFOSR-TR-83-0666 F/G 9/4 NL

END

DATE FILMED

9 - 83

DTIC

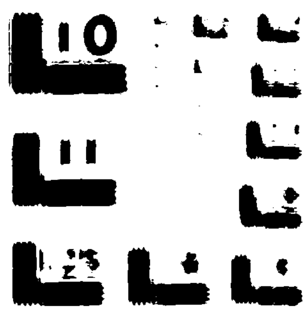

REPORT DOCUMENTATION PAGE

READ INSTRUCTIONS BEFORE COMPLETING FORM

1. REPORT NUMBER

AFOSR-TR- 83-0666

2. GOVT ACCESSION NO.

3. RECIPIENT'S CATALOG NUMBER

DD FORM 1473

[illegible]

[illegible]

[illegible]

AFOSR-TR- 83-0666

[illegible]

[illegible]

[illegible]

[illegible]

by

[illegible]*

[illegible]

[illegible]

[illegible]

*[illegible]

83 08 08 165

THE EFFECT OF SMALL NOISE ON IMPLICITLY DEFINED NON-LINEAR DYNAMICAL SYSTEMS

Abstract

The dynamics of a large class of non-linear systems are described implicitly, i.e. as a combination of algebraic and differential equations. These dynamics admit of jump behavior. We extend the deterministic theory to a stochastic theory since (i) the deterministic theory is restrictive, (ii) the macroscopic deterministic description of dynamics frequently arises from an aggregation of microscopically fluctuating dynamics and (iii) to robustify the deterministic theory. We compare the stochastic theory with the deterministic one in the limit that the intensity of the additive white noise tends to zero. We study the modelling issues involved in applying this stochastic theory to the study of the noise behavior of a multivibrator circuit, discuss the limitations of our methodology for certain classes of systems and present a modified approach for the analysis of sample functions of noisy non-linear circuits.

Keywords: Bifurcation, Singular Perturbation, Jump Behavior, Laplace's method, Noise behavior of non-linear circuits.

Section 1. Introduction

The dynamics of a large class of engineering systems are described only implicitly, for instance, those of non-linear circuits,swing dynamics of an interconnected power system, as also thermodynamic systems far from equilibrium. The implicit definition of their dynamics is as follows: the state variables are constrained to satisfy some algebraic equations, i.e. they are constrained to lie on a manifold M in the state space. The dynamics on this manifold M are then specified implicitly by specifying only the projection of the vector field on M onto a certain base space above which M lies. (i.e. a subspace of the original state space of the same dimension as M). The process of obtaining the system dynamics explicitly consists of 'lifting' the specified velocities onto a vector field on M (lifting is the inverse of projecting). Lifting may not, however, be possible at points where the projection map (restricted to the tangent space of the constraint manifold) has singularities. This singularity is typically resolved by <u>regularization</u>, i.e. by interpreting the algebraic constraint equations as the singularly perturbed limit of 'parasitic' or fast dynamics. The dynamics of the original system are obtained as the degenerate limit of the dynamics of the regularized system - the resulting trajectories may be discontinuous and this is referred to as <u>jump behavior.</u>

The foregoing deterministic theory needs to be extended to a stochastic theory for three reasons:

a) The conditions under which the limit trajectories to the regularizations exist are extremely restrictive so as to exclude several systems of interest.

b) Frequently, the algebraic constraint equations arise from the macroscopic aggregation of microscopically fluctuating dynamics, e.g. the flow of current in a resistor, the demand for electrical power at a distribution point in an electrical power network. More generally, deterministic equations describing thermodynamic systems are of this kind. Thus, the algebraic constraint equations contain in addition a rapidly fluctuating (or white noise) component.

c) The methods of analysis for deterministic systems of the implicitly defined kind involve techniques of bifurcation theory - their conclusions are extremely sensitive to imperfections and the addition of white noise.

Since in all the situations of interest to us, the intensity of the additive noise is small, we study in this paper the dynamics of implicitly defined dynamics in the presence of small additive noise. In fact, we compare the conclusions of the stochastic theory with those of the deterministic theory in the limit that the noise intensity tends to zero. The foregoing process requires the computation of two sets of limits: the limit that the regularization tends to zero and the limit that the intensity of the additive white noise tends to zero. In general, these limits do not commute. We explore in this paper the modelling issue of which sequence of limits is appropriate in the context of a specific system. The layout of the paper where we carry out this program is as follows:

In Section 2, we review briefly the dynamics of deterministic constrained systems and their jump behavior. With some minor modifications we follow here our earlier work [11] and the references contained therein.

In Section 3, we begin the study of noisy constrained dynamical systems. For the initial study we use as tools the work of Papanicolaou, et al [10] on martingale approaches to limit theorems. To study the

dynamics of noisy constrained systems in the presence of small noise, we develop and use in our context Laplace's method of steepest descent. We study in several separate cases, the comparison between the deterministic and small noise theory, describing: (i) how the stochastic theory yields conclusions about system dynamics when the deterministic theory fails and (ii) how the jump behavior of systems is modified by the presence of small noise. This section is a considerable extension of our previous work in the context of phase transitions in van der Vaals gases [12]. Several examples are presented to instantiate our results.

In Section 4, we present the detailed deterministic analysis of Section 2 applied to the dynamics of an emitter coupled relaxation oscillator circuit. We then show that the experimental conclusions of Abidi [1] on the dynamics of these circuits in the presence of small noise seem not to agree with the stochastic theory presented in Section 3.

In Section 5, we discuss the sequences of limits implied by the development of Section 3 - and the nature of systems for which this development yields the correct conclusions. In particular, we show that the development of Section 3 is relevant to systems where the separation in time scales between the slow and fast components is very large and is more important than the small intensity of the white noise (characterized by a certain sequence of limits subsumed by Section 3) - for instance in phase transitions, reaction rates and other phenomena of non-equilibrium thermodynamics. For non-linear circuits, however, the separation in time scales is less marked, so that we present here the relevant analysis (sample function calculations) for these systems with the order of limits reversed from that of Section 3. We use as tools the foundational

work of [illegible] systems. We [illegible] experimental conclusions of Section [illegible].

In Section 5, we discuss suggestions for future work. The present paper clearly is only a beginning [illegible] and modelling problems associated with the dynamics of [illegible] linear systems, such as nonlinear circuits. [illegible] present work will eventually help in formulating [illegible] phenomenological behavior of nonlinear circuits in the presence of noise. This is a topic of great interest [illegible] where noise will play a [illegible] role [illegible].

[illegible]

[illegible]

[illegible]

[illegible]

[illegible]

[illegible]

[illegible]

[illegible]

[illegible]

[illegible]

[illegible] are then interpreted [illegible]

[illegible] well defined system [illegible]

[illegible]

[illegible] the

[illegible]

[illegible]

The intuitive picture that now emerges in the original t-timescale is as follows: For a hyperbolic equilibrium point (x_o, y_o) of the sped-up system $\mathcal{S}$ attach its stable manifold $S_{y_o}^{x_o}$ transversally to M. When the attached manifold $S_{y_o}^{x_o}$ is of dimension m , then disturbances and noise will not cause the "state" (x,y) of the system (2.1), (2.2) to be repelled from M. If, in fact, the attached manifold is of dimension < m, disturbances may cause the "state" (x,y) to be repelled from M and follow instantaneously the dynamics of the sped-up system $\mathcal{S}$ to a new [illegible]-limit set of (2.8). By <u>assuming</u> that [illegible] has only finitely many equilibrium points as its [illegible] limit sets for each x, we may guarantee that (x,y) will [illegible] a new equilibrium point of $\mathcal{S}$. [illegible] unstable it is likely that the [illegible] will [illegible] till a new stable equilibrium point is reached.

[illegible] with respect [illegible]

[illegible]

[illegible] $\mathcal{S}$ [illegible] -limit sets, [illegible] assumption.

[illegible] we <u>assume</u> that the only [illegible] equilibrium points [illegible] $\mathcal{S}$ has are those which have eigenvalues at the origin rather [illegible] singular [illegible] Hopf bifurcation, [illegible] bifurcation [illegible] of $\mathcal{S}$. Several possibilities [illegible] argument [illegible]

[illegible]

[illegible]

[illegible]

[illegible]

[illegible]

[illegible]

[illegible]

[illegible]

[illegible]

[illegible]

[illegible]

[illegible]

[illegible]

[illegible]

[illegible]

[illegible]

[illegible]

[illegible]

[illegible]

[illegible]

[illegible]

[illegible]

[illegible]

[illegible]

[illegible]

[illegible]

[illegible]

[illegible]

[illegible] of equation [illegible]

We now proceed to compare [illegible]-constrained systems with deterministic constrained systems.

3.1 Constrained Dynamical Systems in the Presence of Small Driving Noise

Frequently the model (3.1), (3.4) of noisy constrained systems differs from the deterministic model (2.1), (2.4) in only a small way — i.e. the variances [illegible], scaling ξ and [illegible] in equations (3.1) and (3.4) respectively are small. In the circuit context, as we shall show in the next section, [illegible] and [illegible] are of order of kT where k is the Boltzmann constant and T the temperature in degrees Kelvin, a quantity that is small at room temperature. Thus, we compare the behavior of noisy constrained dynamical systems with that of the deterministic constrained systems of Section 2 in the limit that [illegible], the variances of the driving noise go to zero. The major tools used are Laplace's method of steepest descent for asymptotic calculations (see e.g. Chap. 4 of [illegible] [illegible]), the techniques of Papanicolaou et al. [illegible], and the results of Ventsel-Freidlin [illegible]. The development is of several stages depending on the form of $g(\cdot)$.

3.2 The Case of a Gradient Constraint Equation

Assume that $g(x,y)$ is the gradient with respect to y of a function $S(x,y)$, i.e.

$$g(x,y) = -\frac{\epsilon}{2}\,\mathrm{grad}_y\, S(x,y)$$

for some function $S : \mathbb{R}^n \times \mathbb{R}^m \to \mathbb{R}$. Then, the results of Papanicolaou, et al. [illegible] yield that provided the derivatives of S with respect to y grow rapidly enough at ∞, the density of the diffusion generated by (3.4) converges exponentially to

$$\bar{p}^{\epsilon}(x,y) = c^{\epsilon}(x)\cdot\exp\left(-\frac{S(x,y)}{\epsilon}\right) \qquad (3.20)$$

where $c^{\epsilon}(x)$ is chosen such that

$$\int_{\mathbb{R}^m} \bar{p}^{\epsilon}(x,y)\,dy = 1$$

Note that for all $\lambda>0$ and $x \in \mathbb{R}^n$ the critical points (with respect to y) of $\bar{p}^{\lambda}(x,y)$ are the equilibrium points of the deterministic system (2.4) with x frozen given in this instance by

$$\dot{y} = -\frac{1}{2}\,\mathrm{grad}_y\, S(x,y) \quad . \tag{3.11}$$

Further, if for some x_o, $S(x_o,y)$ is a Morse function (of y), then for all $\lambda > 0$ every local maximum of $\bar{p}^{\lambda}(x,y)$ is a stable equilibrium of (3.11).

To compare the noisy constrained system with the deterministic constrained system in the limit that $\lambda \downarrow 0$, it will be necessary to evaluate integrals like (3.9) in the limit that $\lambda \downarrow 0$. This is done using the following version of Laplace's method:

Theorem 3.2 (Laplace's Method)

Let for each $x \in \mathbb{R}^n$, $S(x,y)$ have global minima at $y_1^*(x)$, $y_2^*(x), \ldots y_N^*(x)$, where N may depend on x. Let them all be non-degenerate.[1] Further, let $S(x,y)$ have at least quadratic growth (in y) as $y \to \infty$. Then, in the limit that $\lambda \downarrow 0$, $\bar{p}^{\lambda}(x,y)$ converges to

$$\sum_{i=1}^{N} a_i(x)\, \delta(y - y_i^*) \Big/ \sum_{i=1}^{N} a_i(x)$$

where $a_i(x) = \det(D_2^2\, S(x,y_i^*(x)))^{-1/2}$ (3.12)

More precisely, if $\phi(x,y)$ is a smooth function having polynomial growth as $y \to \infty$, then

$$\begin{aligned}\lim_{\lambda \downarrow 0} \bar{\phi}_{\lambda}(x) &= \lim_{\lambda \downarrow 0} \int_{\mathbb{R}^m} \phi(x,y)\, \bar{p}^{\lambda}(x,y)\,dy \\ &= \sum_{i=1}^{N} a_i(x)\, \phi(x,y_i^*(x)) \Big/ \sum_{i=1}^{N} a_i(x) \qquad (3.13) \\ &= \bar{\phi}_o(x)\end{aligned}$$

[1] i.e. the Hessian $D_2^2\, S(x,y)$ at $y = y_i^*(x)$ is nonsingular

Proof: Since $\bar{p}^{\lambda}(x,y) = \exp - \frac{S(x,y)}{\lambda} \Big/ \left[\int_{\mathbb{R}^m} \exp - \frac{S(x,y)}{\lambda} dy\right]$,

we will first evaluate

$$\int_{\mathbb{R}^m} \phi(x,y) \exp - \frac{S(x,y)}{\lambda} dy$$

for simplicity first assume that $S(x,y)$ has a single global minimum at $\hat{y}$. We will then show that

$$\int_{\mathbb{R}^m} \phi(x,y) \exp - \frac{S(x,y)}{\lambda} dy = \phi(x,y^*) \frac{(2\pi\lambda^{m/2}) \exp - S(x,y^*)/\lambda[1 + o(1)]}{[\det D_2^2 S(x,y^*)]^{1/2}} \tag{3.14}$$

First, by the Morse Lemma (see for e.g. Milnor [16]) there exists a neighborhood U of $\hat{y}$ and a change of coordinates $\mathbb{R}^m \to U$ given by $y = \gamma(\bar{y})$ such that $y^* = \gamma(0)$ and

$$S(x,y) = S(x,y^*) + \frac{1}{2} \sum_{i=1}^{m} (\bar{y}_i)^2 \tag{3.15}$$

Further, outside the neighborhood U of y^*, $S(x,y) > S(x,y^*) + \delta$ for some $\delta > 0$ so that

$$\int_{\mathbb{R}^m/U} \phi(x,y) \exp - \frac{S(x,y)}{\lambda} dy = \exp\left[\frac{-S(x,y^*)}{\lambda}\right] o(\lambda^{\delta}) \tag{3.16}$$

for all $\lambda > 0$. Clearly, then (3.16) does not contribute to the leading term of (3.14) Consider now

$$\int_U \phi(x,y) \exp - \frac{S(x,y)}{\lambda} dy$$

$$= \exp - \frac{S(x,y^*)}{\lambda} \int_{\mathbb{R}^m} \exp\left(-\sum_{i=1}^{m} \bar{y}_i^2\right) \phi(x,\gamma(\bar{y})) |\det D\,\gamma(\bar{y})| d\bar{y} \tag{3.17}$$

Now, standard manipulations with Gaussian distributions yield that

$$\int_{\mathbb{R}^m} (\exp - \frac{1}{2\lambda} \sum_{i=1}^{m} \bar{y}_i^2)\, \phi(\bar{y})\, d\bar{y}$$

$$= (2\pi\lambda)^{m/2} (\phi(0) + o(\lambda)) \tag{3.18}$$

Thus, to evaluate (3.17) we only need compute $|\det D\,\gamma(0)|$. Differentiating (3.15) twice with respect to y yields

$$D_2^2\, S(x,y) = ((\frac{d\bar{y}}{dy})^{-1})^T (\frac{d\bar{y}}{dy})^{-1} . \tag{3.19}$$

From (3.19) it follows that

$$|\det D\,\gamma(0)| = [\det D_2^2\, S(x,y^*)]^{-1/2}$$

so that (3.14) now is immediate on combining (3.16), (3.17) **and (3.18)**

In the instance that $S(x,y)$ has several global minima $y_1^*(x), y_2^*(x), \ldots, y_N^*(x)$ it follows from an easy extension of the foregoing argument that

$$\int_{\mathbb{R}^m} \phi(x,y) \exp - \frac{S(x,y)}{\lambda} dy = (2\pi\lambda)^{m/2} \exp \frac{-S(x,y^*)}{\lambda} [\sum_{i=1}^{N} \det [D_2^2\, S(x,y_i^*(x))]^{-1/2}$$

$$\phi(x,y_i^*(x)) + o(1)] \tag{3.20}$$

Selling $\phi(x,y) = 1$ in (3.20) yields the corresponding expression for $\int_{\mathbb{R}^m} \exp \frac{-S(x,y)}{\lambda} dy$. Combining this with (3.20) we have equation (3.13).

$\square$

<u>Remarks:</u> (1) If the growth conditions on $S(x,y)$ and $\phi(x,y)$ are uniform in x for $|x| \leq R$ it can be shown that for $p \geq 1$

$$\int_{|x|\leq R} |\bar{\phi}_\lambda(x) - \bar{\phi}_0(x)|^p\, dx \to 0 \quad \text{as } \lambda \downarrow 0 \tag{3.21}$$

Proof: Is presented in Sastry-Hijab [12].

Remark: The order of the limits is peculiar in Theorem (3.3). If the order is interchanged i.e. $\lambda \downarrow 0$ first and then $\varepsilon \downarrow 0$ it is clear that one recovers in the limit the deterministic development of Section 2 (with the minor modification that $\dot{x}$ has an additive white noise terms. The jump-behavior or the y-variable is as explained in that section. If, however, $\varepsilon \downarrow 0$ first and the $\lambda \downarrow 0$, the jump-behavior of the y-variable is somewhat different, as we now elaborate:

The behavior of the conditional density of y given x as $\lambda \downarrow 0$ is as in Theorem 3.2: the y variable is at one of the global minima of $S(x,\cdot)$ with probability proportional to the curvature of $S(x,\ )$ $((\mathrm{Det}\ D_2^2\ S(x,y_i^*))^{-1/2})$ at that minimum. Consider first the case when the minimum is unique. There is then a jump in the y-variable if there is a change in the global minimum of $S(x,\cdot)$ as x is varied. Points of jump then will be points of appearance and disappearance of global minima of $S(x,\cdot)$. This is in contrast to the deterministic picture of Section 2, where, for the instance that $g(x,y)$ is of the form of (3.11), stable equilibrium of the sped-up system S are local minima of $S(x,\cdot)$ and points of bifurcation are points appearance and disappearance of local minima of $S(x,\cdot)$.

We illustrate this with an example - the van der Pol oscillator of (2.5), (2.6) with added noise. Consider

$$\dot{x} = y + \sqrt{u}\ \xi(t)$$
$$\varepsilon \dot{y} = -x - y^3 + y + \sqrt{\lambda\varepsilon}\ \eta(t)$$

Here $S(x,y) = -xy - \frac{y^4}{4} + \frac{y^2}{2}$ so that, in the limit that $\varepsilon \downarrow 0$; the x-process converges to one satisfying

The proof of (3.22) uses the dominated convergence and [illegible] theorem.

(2) If $S(x,y)$ has a manifold M of global minima, then [illegible] these global minima cannot be non-degenerate. However if [illegible] is non-degenerate in directions orthogonal to M, then a minor modification of the preceding theorem yields

$$\int_{\mathbb{R}^m} \exp\left(\frac{-S(x,y)}{[illegible]}\right) [illegible]\, dy$$
$$= [illegible]^{m/2}\, e^{-S(x,\hat{y})/[illegible]} \int_M \frac{[illegible]}{H(x,\cdot)}\, d\sigma_M + [illegible]$$

Where $\hat{y}$ is any point belonging to M, $H(x,\cdot)$ is the determinant of the non-degenerate part of the Hessian and $d\sigma_M$ is the [illegible] measure [illegible].

We can now combine the results of Theorems [illegible] and [illegible], using a minor modification of the techniques of [illegible].

<u>Theorem 3.3</u> Weak convergence of [illegible].

Given any T [illegible], in the limit that [illegible], the first component $x(t)$ of the solution [illegible] converges weakly in $C([0,T];\mathbb{R}^n)$ to the unique diffusion [illegible] satisfying [illegible] law

$$\dot{x} = \bar{f}_0(x) + [illegible] \quad [illegible]$$

where

$$\bar{f}_0(x) = \sum_{i=1}^{N} a_i(x)\, f(x, y_i^*(x)) \Big/ \sum_{i=1}^{N} a_i(x) \quad [illegible]$$

and the $y_1^*(x),\ldots,y_N^*(x)$ are the non-degenerate global minima of $S(x,\cdot)$ and $a_i(x) = [\det D_2^2 S(x, y_i^*(x))]^{-1/2}$.

[illegible]

$$[illegible]$$

[illegible]

[illegible]

[illegible]

$$[illegible]$$

[illegible]

[illegible]

$$[illegible]$$

[illegible]

[illegible]

[illegible]

[illegible]

[illegible]

[illegible] system. However, it [illegible] example [illegible]

[illegible]

[illegible] "[illegible]" features [illegible]

[illegible]

[illegible]

[illegible]

[illegible]

[illegible]

[illegible]

[illegible]

[illegible]

[illegible]

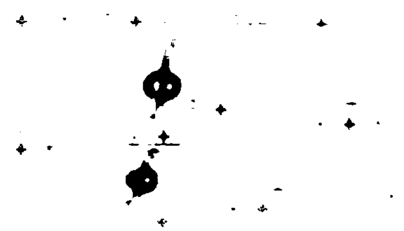

[illegible]

[illegible]

[illegible]

[illegible]

[illegible]

[illegible]

[illegible]

[illegible]

[illegible]

[illegible]

[illegible]

[illegible]

Section 4 The Effects of Thermal Noise on an Emitter-Coupled Relaxation Oscillator

We study in this section the relevance of the theory developed in Sections 2 and 3 to the study of the effects of thermal noise on a relaxation oscillator. Figure 9 shows a simplified circuit diagram of such an oscillator, the Analog Devices AD 537. We discuss first using the terminology of Section 2 the deterministic description of the oscillator. The circuit equations are given by

[illegible] (4.1)

[illegible] (4.2)

[illegible] (4.3)

[illegible] (4.4)

[illegible] (4.5)

Here $V_T = \frac{kT}{q}$ is the threshold voltage for the base emitter junction and I_s is the reverse saturation current. The transistors are assumed to be identical. With $v = V_{e1} - V_{e2}$, we may combine equations (4.2) - (4.5) to obtain

$$\frac{d}{dt} v = \frac{1}{C} (I_0 + i) \tag{4.6}$$

$$0 = v - (2I_0 + 2i)R - V_T \ln \frac{2I_0 - i}{i} \tag{4.7}$$

Equations (4.6), (4.7) form an implicitly defined dynamical system. The solution set of the algebraic equation (4.7) is plotted in the (v,i)

plane in Figure 10. Some of the features of this curve are noted below:

(i) For $-2I_0R < V < 2I_0R$ the equation (4.7) has three solutions, while for $V > 2I_0R$ and $V < -2I_0R$ the equation has only one solution.

(ii) As $V \to \infty$, $i \to 2I_0$ and as $V \to -\infty$, $i \to 0$ asymptotically.

(iii) The values $V \cong 2I_0R$, $i \cong \frac{V_T}{2R}$ and $V \cong -2I_0R$, $i \cong 2I_0 - \frac{V_T}{2R}$ are the points of bifurcation of equation (4.7) with V treated as the bifurcation parameter, i.e. at these points it is not possible to solve (4.7) for i as a function of V locally and uniquely. These points may be shown to be points of fold bifurcation.

Returning now to the full system - (4.6) and (4.7) we see that continuous solutions for the system exist so long as i can be solved continuously as a function of V in (4.7) so as to obtain:

$$\frac{dv}{dt} = \frac{I_0 - i}{C} \qquad (4.6)$$

and

$$\frac{di}{dt} = \frac{(I_0 - i)/C}{-2R + V_T \cdot 2I_0/((2I_0 - i)i)} \qquad (4.8)$$

When $-2R + V_T \cdot 2I_0/((2I_0 - i)i) = 0$, i.e. $i = V_T/2R$ or $i = 2I_0 - V_T/2R$ it appears that $\frac{di}{dt}$ is infinite so as to prevent the integration of equations (4.6), (4.8). The regularization of this system is accomplished by taking into account the fact that parasitic capacitances present in the transistors, as well as the finite slew rate of the operational amplifiers will prevent i from varying discontinuously and in effect change the description of the

of the circuit dynamics from (4.6), (4.7) to

$$C\frac{dV}{dt} = \frac{(I_0 - i)}{C} \tag{4.6}$$

$$\varepsilon \frac{di}{dt} = V - (2I_0 - 2i)R - V_T \ln (2I_0 - i)/i \tag{4.9}$$

Equations (4.6) and (4.9) are a gross simplification of all the actual parasitics present in the circuit. A more detailed and exhaustive description involving all the parasitics would start from the original equations (4.1) - (4.5). The present regularized model is, however, accurate enough for our purposes. The phase portrait of this system shown in Figure 1 includes a single unstable equilibrium point ($V=0$, $i=I_0$) and a limit cycle. The limit trajectories of (4.6), (4.9) as $\varepsilon \downarrow 0$ exist and include the relaxation oscillation shown in Figure 12 - a limit cycle with two discontinuities - at the points where the trajectory switches from the Q1 on, Q2 off 'state' to the Q1 off, Q2 on 'state' and vice versa. Note also from Figure 11 that the Q1 on, Q2 on 'state' is unstable as evidenced by the trajectories of (4.6), (4.9) pointing away from that 'state'. The current waveform $i(t)$ is as shown in Figure 13. The half period of the oscillation T may be estimated approximately by integrating equation 4.8 with the approximation that for $0 \le t \le T$, $i \ll I_0$, so that we have

$$T \cong \frac{C}{I_0} \int_{I_1}^{V_T/2R} \left(-2R + \frac{V_T}{i}\right) di$$

or

$$T \cong \frac{C}{I_0} \left[2R(-V_T/2R + I_1) + V_T \ln (V_T/2I_1R)\right] \tag{4.10}$$

From equation (4.10) it follows that the frequency of oscillation is (approximately) lienarly proportional to I_0, which enables this oscillation to be used as an electronically tunable oscillator (e.g. in a phase locked loop). In such applications, it is important to know the noise characteristics of the oscillator in response to resistive thermal noise. Experimental observations of Abidi [1] indicate that the actual (noisy) current waveform is as shown in Figure 14. Key features of this figure are as follows:

(a) the transitions or jumps appear to be noise free

(b) the noise superimposed on the deterministic waveform of Figure 13 appears to be small (low intensity) immediately following a jump and then appear to build in intensity.

We assume (see e.g.[14]) that all the noise sources in the circuit can be lumped into a single-noisy current source $i_n(t)$ shown dotted in Figure 9: $i_n(t)$ is assumed to be white with intensity λ(with λ small at room temperatures, since it is proportional to kT). It is easy to check that the equation (4.6) is now unchanged, while (4.7) changes to

$$0 = V - (2I_0 - 2i)R - V_T \ln(2I_0 - i)/i + 2R\sqrt{\lambda}\, i_n(t) \tag{4.11}$$

We regularize the system (4.6), (4.11) as before to obtain

$$\dot{V} = (I_0 - i)/C \tag{4.6}$$

$$\varepsilon\dot{i} = V - (2I_0 - 2i)R - V_T \ln(2I_0 - i)/i + 2R\sqrt{\varepsilon\lambda}\, i_n(t) \tag{4.12}$$

Note that ε scales the intensity of the white noise in (4.12) precisely for the same reason as in equation (3.2) of Section 3. The techniques of Section 3.2 may now be used to obtain that as $\varepsilon \downarrow 0$, the V-process converges weakly on $C([0,T];\mathbb{R})$ to one satisfying :

$$\dot{V} = (I_0 - \bar{i}^{\lambda}(V))/C$$

where $\bar{i}^{\lambda}(v)$ is i integrated over the conditional density for i given V,in the limit that $\varepsilon \downarrow 0$, $\bar{p}^{\lambda}(i,v)$. As in the example of Section 3.2, we have in the limit that $\lambda \downarrow 0$, $\bar{p}^{\lambda}(i,v)$ converging to a sequence of delta functions jumping from one leg of the solution curve to (4.7) to the other at $V = 0$. Also, choosing the interval of weak convergence to be large it appears that the relaxation oscillation is borken up.

This analysis is contrary to the experimental evidence of Abidi [1] What has gone wrong? How does one recover the experimental results of Abidi [1]? These are the questions that we taken up next.

Section 5. Sample Function Calculations.

The mathematical reason for the anomaly between the machinery developed in Section 3 and the experimental conclusions of Section 4, is the order of limits $\varepsilon \downarrow 0$ followed by $\lambda \downarrow 0$ in Theorem (3.3). This order of taking limits is suitable for explaining phenomena in several situations in non-equilibrium thermodynamics (for e.g. phase transitions of the kind discussed in Sastry-Hijab [12], Eyring chemical reaction rates, etc. - see for e.g. Nicolis-Prigogine [9], Landauer [6]). In fact, it has been noted by thermodynamicists of the Brussels School that "fluctuations play a crucial role in changing the behavior of systems near bifurcation fronts". However, this order of limits is not fully satisfactory in the circuit context. The reason for this lies in the fact that the order of limits $\varepsilon \downarrow 0$ followed by $\lambda \downarrow 0$ (Theorem 3.3) yields the correct conclusions only when the dynamics of the fast (sped-up) system are much faster than those of the slower x variable. This is so, because, as we state in Section 3.4, Laplace's method of steepest descent picks for the limit values of $\bar{p}^{\lambda}(x,y)$ as $\lambda \downarrow 0$ the most stable ω-limit sets of the underlying deterministic systems. This in turn is consistent with the intuition that in the presence of persistent random perturbation (wide-band in nature) the trajectories of a system will concentrate after sufficiently long periods of time in the vicinity of the most-stable sets. However, the sufficiently long periods of time may be very large indeed. It is possible to show, for example in the gradient case of Section 3.2 that the average time required to excape from a stable equilibrium is of the order of $e^{k/\lambda}$ for some $k>0$ (see for eg. Schuss [15], Ventsel-Freidlin (15]).

By taking limits in the sequence $\varepsilon \downarrow 0$ followed by $\lambda \downarrow 0$, the implication is that ε is smaller than $e^{-k/\lambda}$, i.e. ε is at least $o(e^{-k/\lambda})$, so that the fast system has sufficiently much time to concentrate in the vicinity of its ω-limit sets. This is frequently the situation in non-equilibrium theromodynamics where the slower dynamics are frequently assumed to be 'quasi-static'. In the circuit context, however, the separation of time scales between the slow and fast variable is not as large as is implied by the theorem.

As noted in the remark following Theorem 3.3; if the order of limits is interchanged (i.e. $\lambda \downarrow 0$ and then $\varepsilon \downarrow 0$), one recovers the deterministic development of Section 2. Before, we further elaborate and make precise the statements of the previous paragraph we indicate how one analyses sample functions of the process generated by (3.1), (3.2) in the limit that $\lambda \downarrow 0$ followed by $\varepsilon \downarrow 0$. The major tool in this development is the work of Ventsel-Freidlin [13].

We consider here sample functions of the process generated by

$$\dot{x} = f(x,y) + \sqrt{\lambda}\,\xi, \qquad x(0) = x_0 \tag{5.1}$$

$$\varepsilon\dot{y} = f(x,y) + \sqrt{\lambda\varepsilon}\,\eta \qquad y(0) = y_0 \ . \tag{5.2}$$

with precisely the same assumptions as in Section 3. Let $\phi = (\phi_x, \phi_y)$: $[0,T] \to \mathbb{R}^n \times \mathbb{R}^m$ be a C^1 map from the interval $[0,T]$ to the x, y space with $\phi_x(0) = x_0$, $\phi_y(0) = y_0$. Define, for this trajectory, the functional $I_\varepsilon(\phi)$ by

$$I_\varepsilon(\phi) = \int_0^T \left\| \begin{matrix} \dot{\phi}_x(t) - f(\phi_x, \phi_y) \\ \varepsilon[\dot{\phi}_y(t) - \frac{1}{\varepsilon} g(\phi_x, \phi_y)] \end{matrix} \right\|^2 dt \ . \tag{5.3}$$

Then, we have the following theorem [illegible] the deviation [illegible] the sample functions [illegible] from the [illegible] specified [illegible]

<u>Theorem</u> [illegible]

For any [illegible] there exists a [illegible] such that

[illegible]

<u>Remarks</u> (1) Equation [illegible] gives an estimate [illegible] the sample functions of the process [illegible] the [illegible] specified [illegible] Clearly, the estimate [illegible] is sharpest when [illegible] We examine this point next.

(2) Consider the definition of [illegible] in equation [illegible] Note that [illegible] is, in fact, the solution [illegible] of the deterministic system starting from x_0, [illegible] then [illegible] its minimum value. Further [illegible] is, for arbitrary [illegible], a measure of how far [illegible] the flow of the deterministic system.

(3) Note the [illegible] weighting in the y-component of equation [illegible]. Taking the limit that [illegible]→0; we see that so long as [illegible] remains bounded the contribution of the second term is merely [illegible].

(4) Note that Theorem 5.1 gives an estimate for the deviation of the process of (5.1), (5.2) from the trajectory [illegible] for fixed [illegible] and [illegible]→0 as follows. For [illegible]→0 with probability arbitrarily close to 1, the most likely trajectory for the process is that which minimizes [illegible]. Further, taking the limit that

[illegible]

[illegible]

[illegible]

[illegible]

[illegible]

[illegible]

[illegible] where

[illegible]

[illegible]

[illegible]

[illegible]

[illegible]

[illegible]

[illegible]

[illegible]

We [illegible] the effect of the addition of small [illegible] system. The [illegible] the dynamics with [illegible] between the time [illegible] of the [illegible] system and the [illegible] derived.

[illegible]

The present paper presents a first step [illegible]

[illegible]

[illegible]

[illegible]

[illegible]

[illegible]

[illegible]

[illegible]

[illegible] and Systems [illegible]

[illegible]

[illegible]

[illegible]

[illegible]

[illegible]

[illegible]

[illegible]

[illegible]

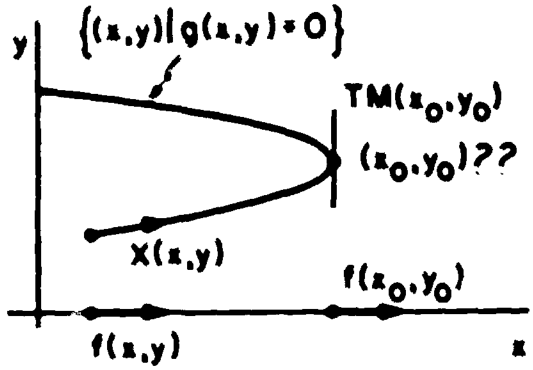

[illegible]

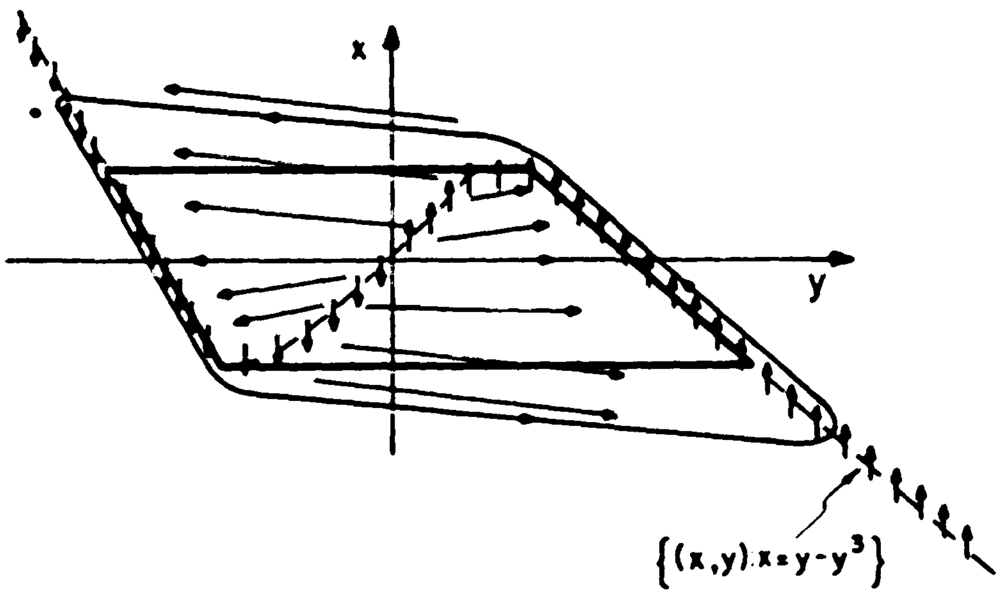

Figure 2: Showing the Dynamics of the Degenerate and Regularized van der Pol Oscillator

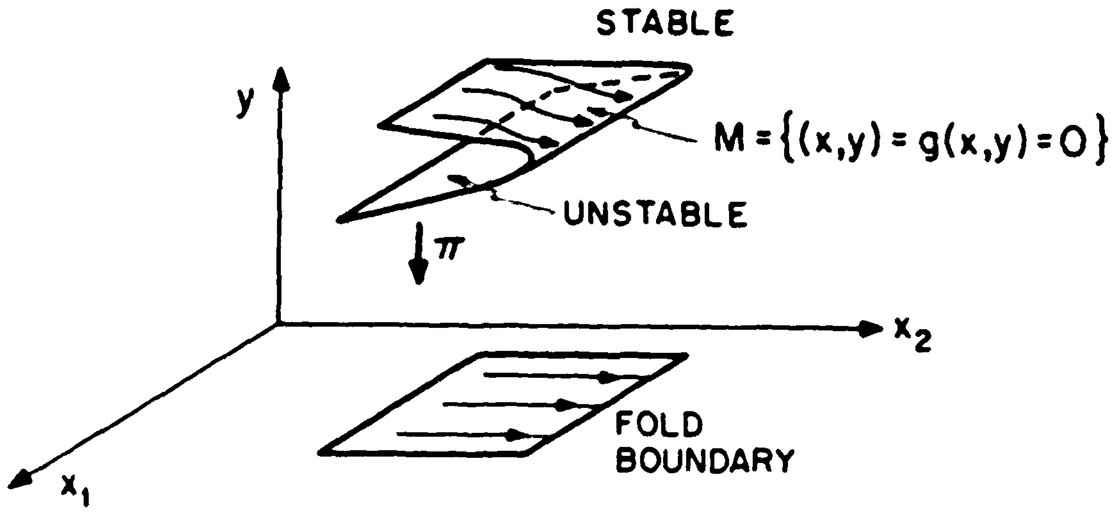

Figure 3: Visualization of a Fold Bifurcation and the Trajectories on M Pointing Toward the Fold Boundary

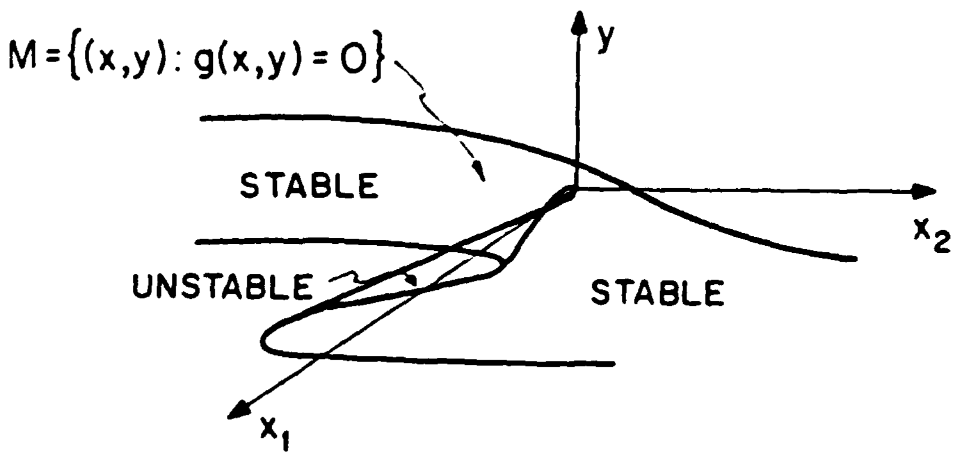

Figure 4: Visualization of a Cusp Bifurcation

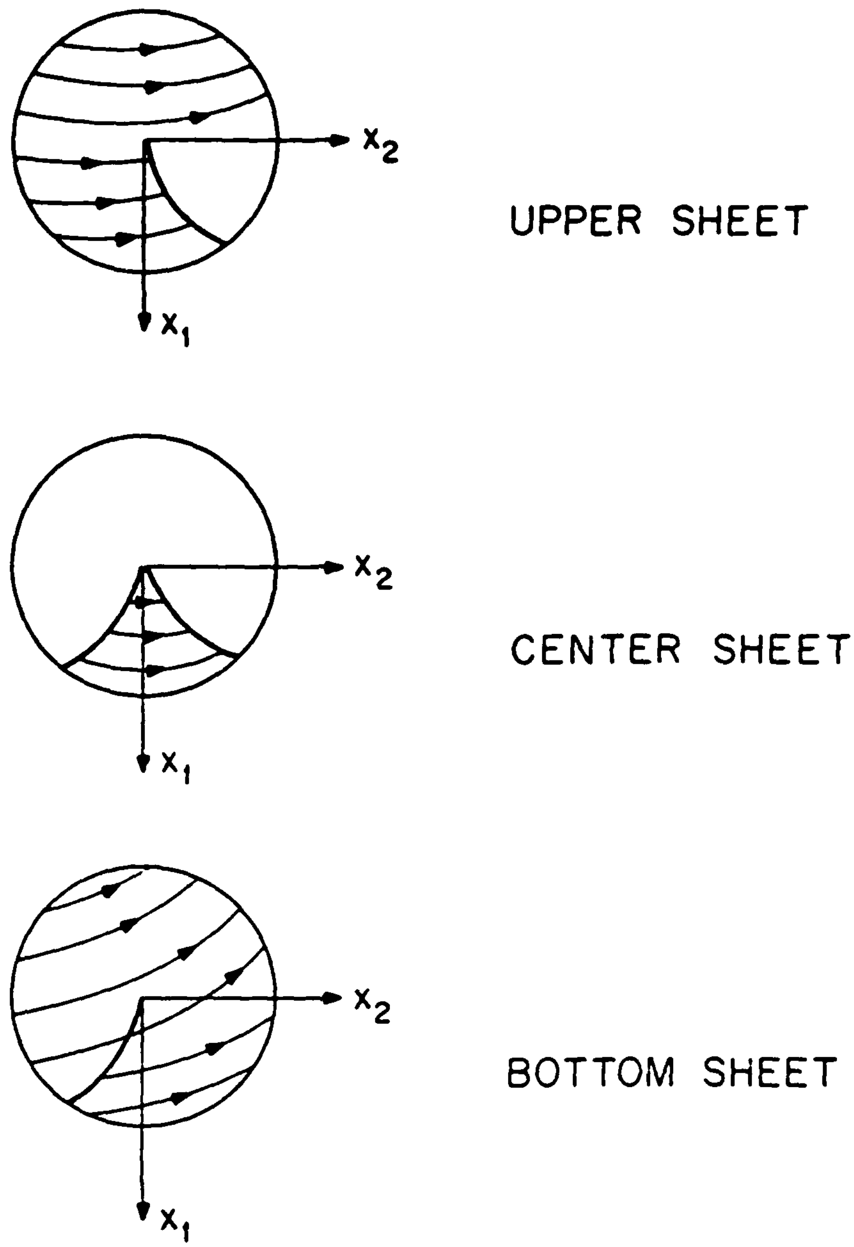

Figure 5: Visualization of the Trajectories on the Upper, Center and Bottom Sheets of the Cusp

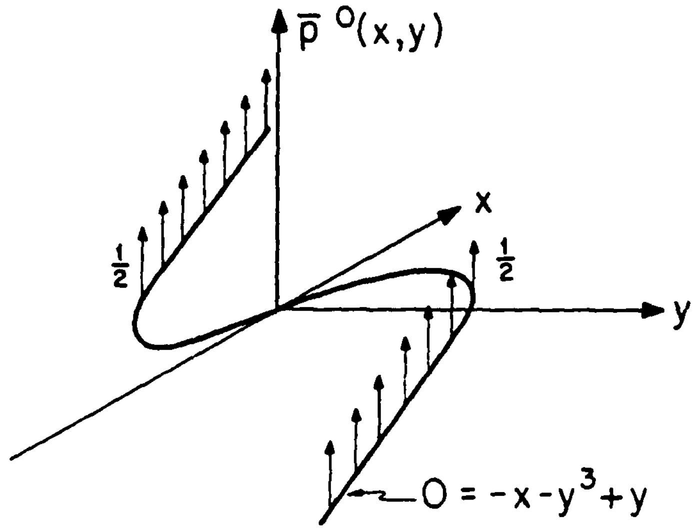

<u>Figure 6</u>: Showing the Limit as $\lambda \downarrow 0$ of the Conditional Density $\bar{p}^{\lambda}(x,y)$

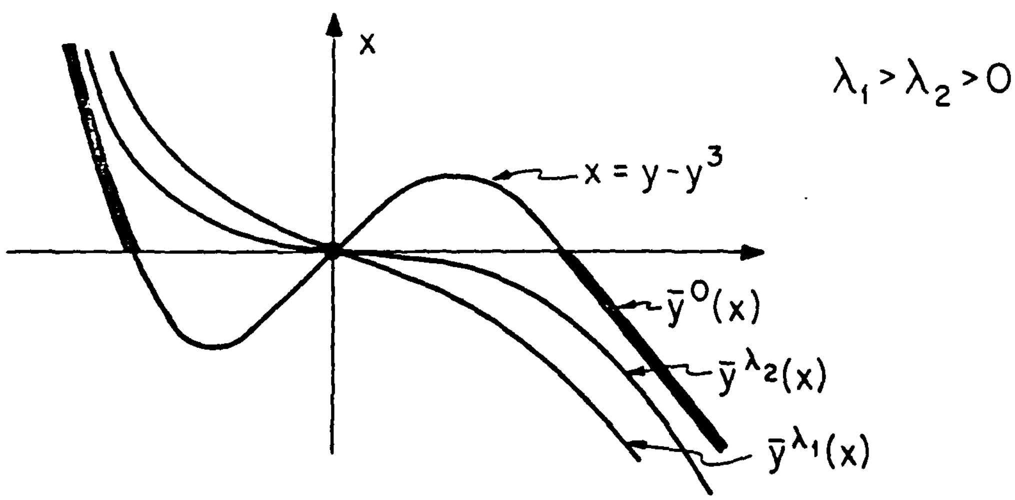

<u>Figure 7</u>: The Drift $\bar{y}^{\lambda}(x)$ for the Limit Diffusion of the van del Pol Oscillator for Decreasing Values of λ.

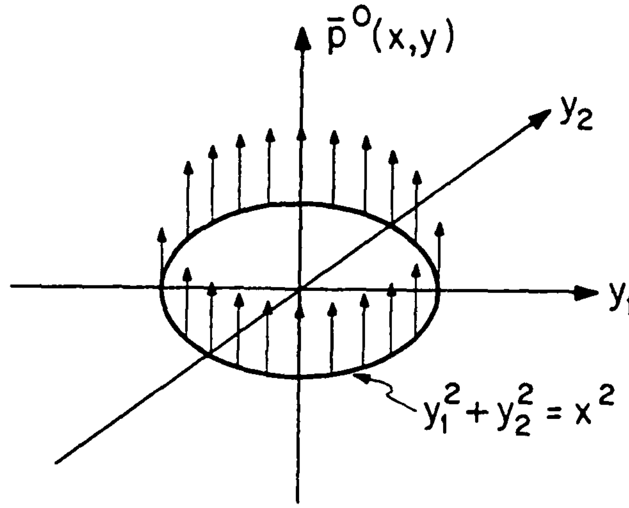

Figure 8: Showing the Limit Behavior of $\bar{p}^{\lambda}(x,y)$ for Example 3.5

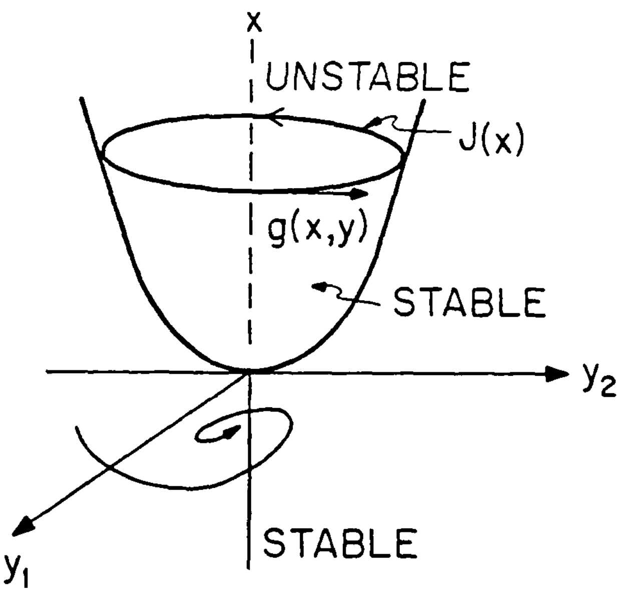

Figure 9: Showing the Hopf Befurcation for the Example 3.6

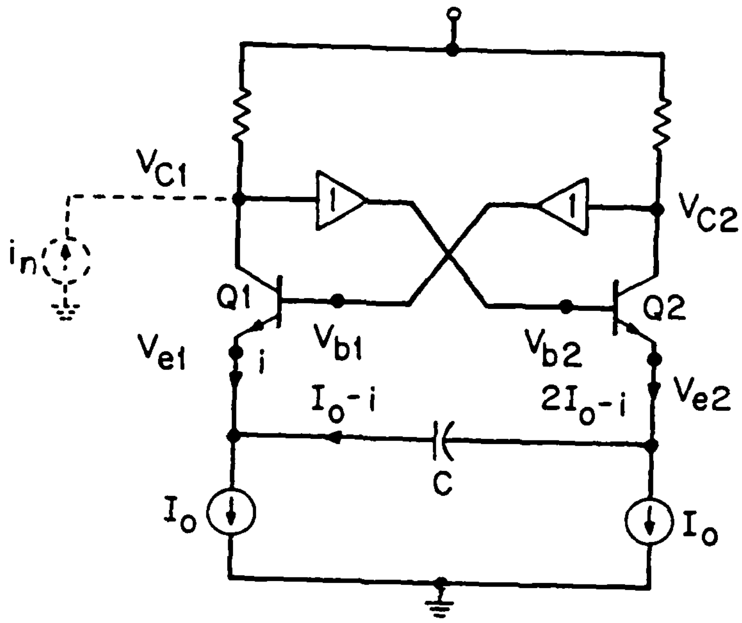

Figure 10: Simplified Circuit Diagram for the Emitter Coupled Relaxation Oscillator

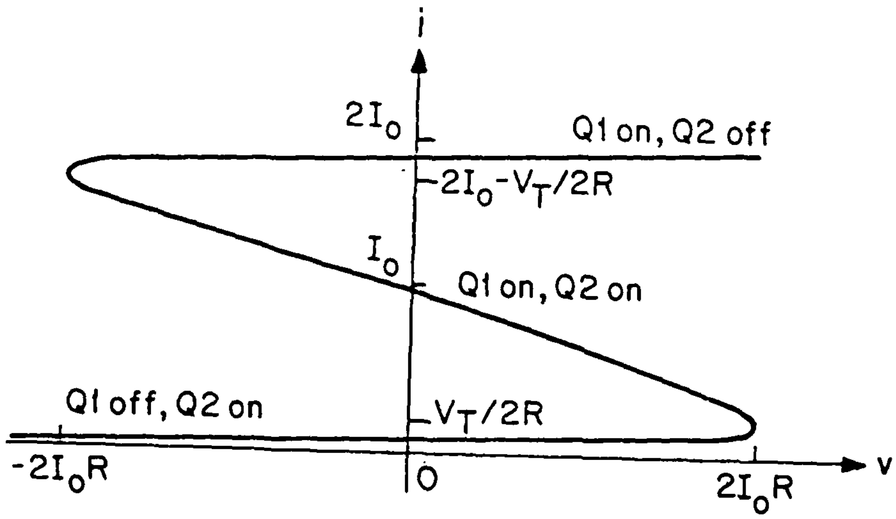

Figure 11: The Solution Curve to the Algebraic Equation (4.7)

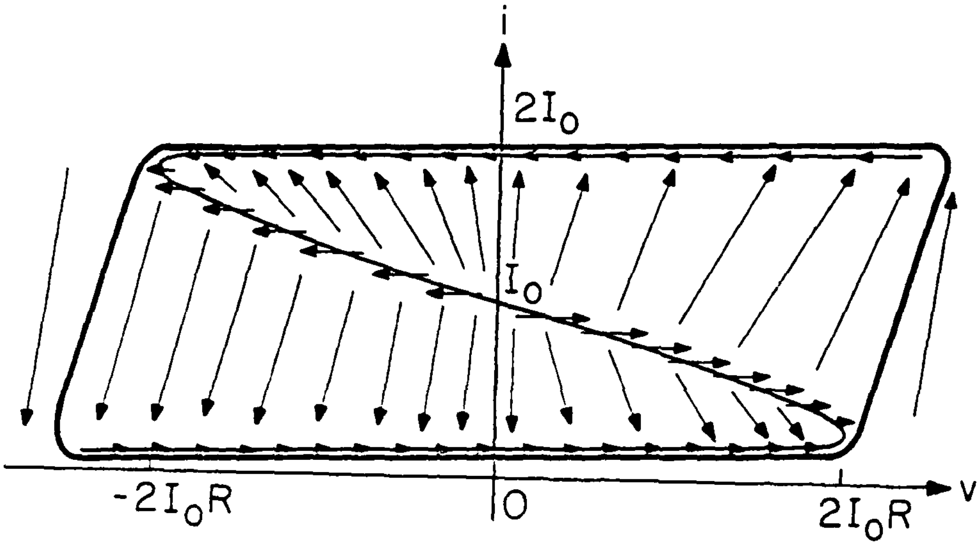

Figure 12: Phase Portrait of the System (4.6) , (4.9)

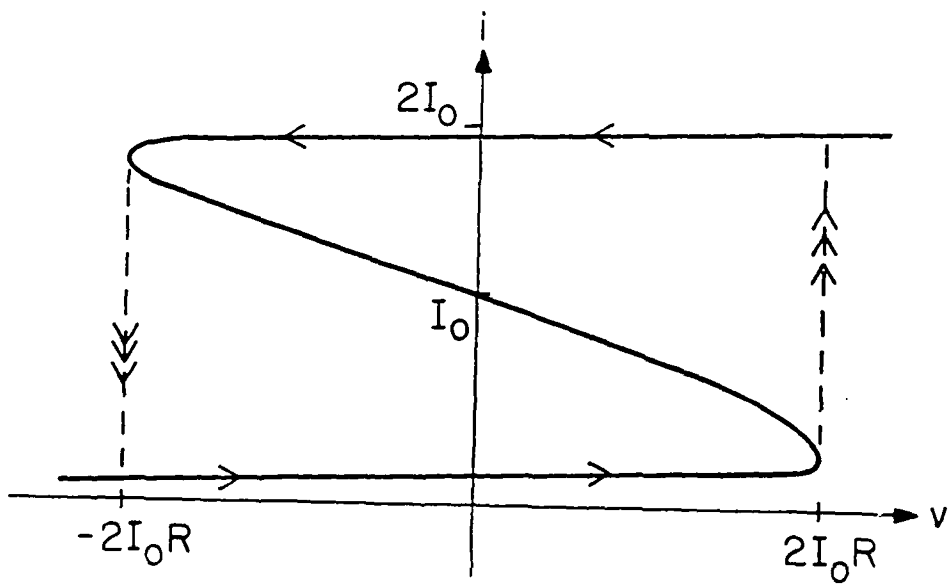

Figure 13: Showing the Relaxation Oscillation in the Emitter Coupled Oscillator

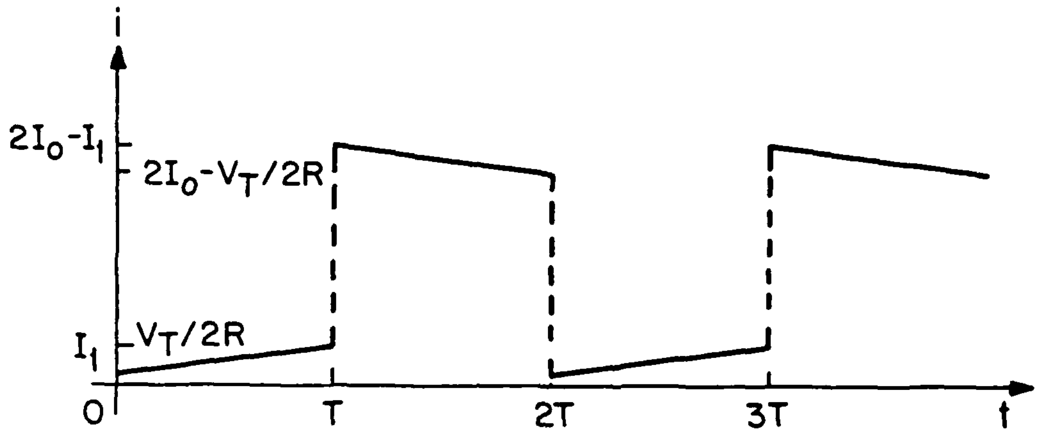

Figure 14: Current Waveform i(t) for the Circuit of Figure 1.

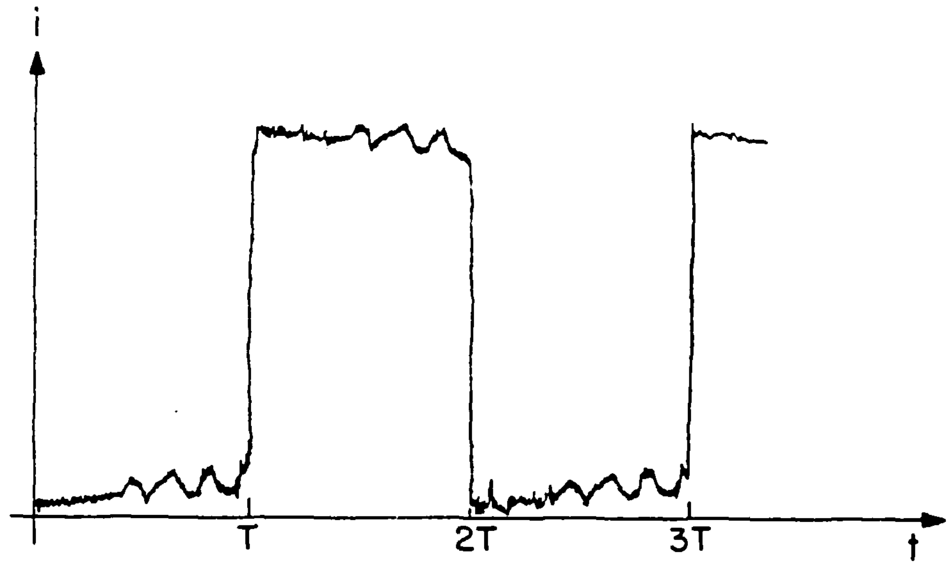

Figure 15: Experimentally Observed Waveform for i(t) in the Presence of Noise (after Abidi[1])

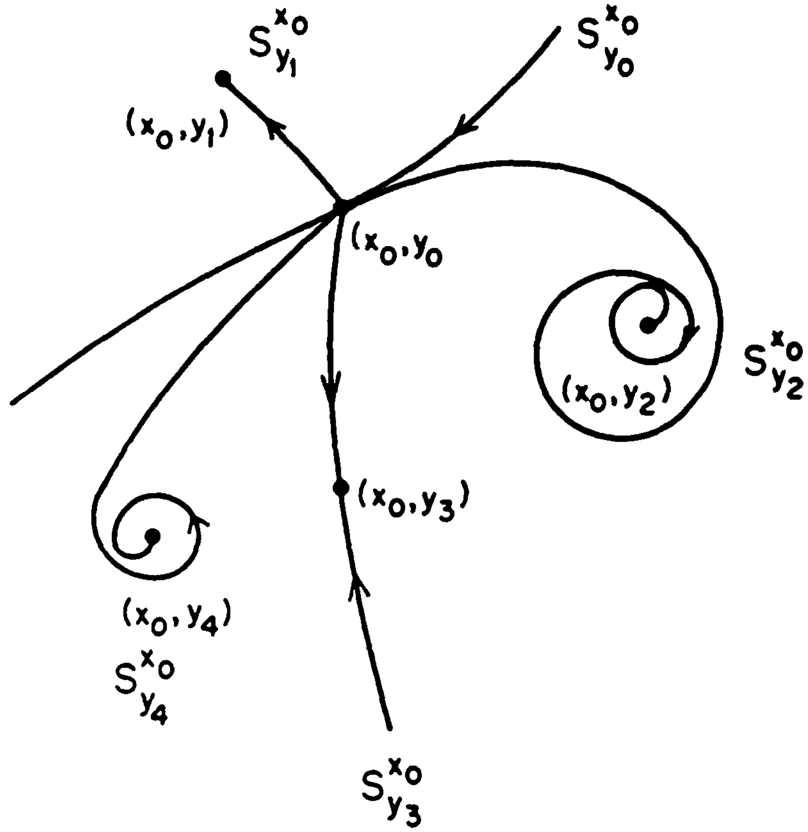

Figure 16: Showing the Possibility of Jump from y_0 to y_1, y_2, y_3 or y_4

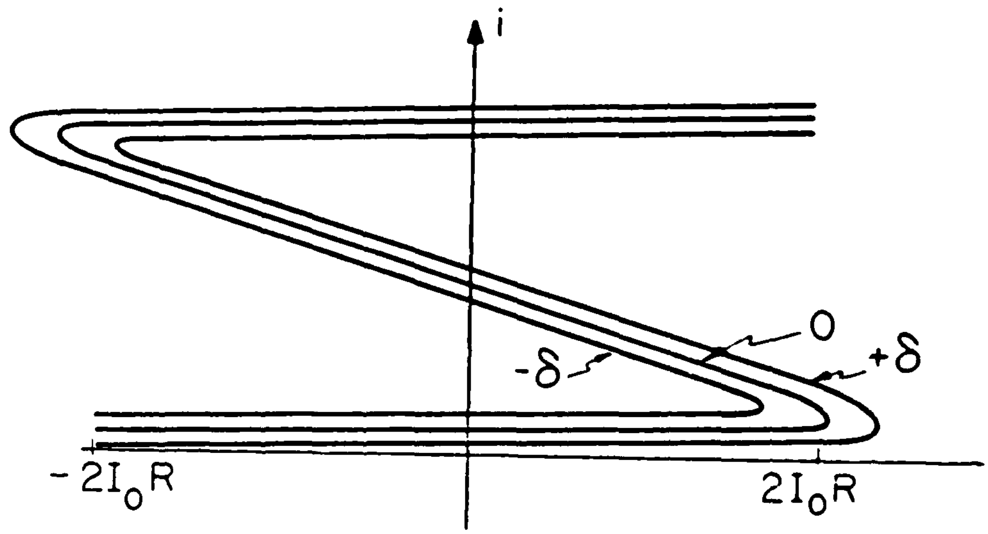

Figure 17: Showing a δ neighbourhood of the Constraint Equation (4.[illegible])

ME

- 8